COMPLETE ANALYTICAL MODEL OF MICROFLUIDIC DIPOLES AND QUADRUPOLES: APPLICATION TO BRUSH STROKE AND GRADIENT CONTROL WITH MICROFLUIDIC PROBES

Thomas Gervais*[1], Mohammadali Safavieh[2], Mohammad Qasaimeh[3], and David Juncker[4]

[1] *Engineering Physics Department, École Polytechnique de Montréal, Montreal, QC, Canada*

[2] *Institut national de la recherche scientifique (INRS), Varennes, QC, Canada*

[3] *New York University Abu Dhabi, Abu Dhabi, United Arab Emirates*

[4] *Biomedical Engineering Department, McGill University, Montreal, QC, Canada,*

ABSTRACT

Microfluidic probes (MFP) are an emerging class of open microfluidic systems that generate precisely controlled flow patterns over an open surface without the need for closed microchannels, with applications in cell studies and surface patterning. Currently, hydrodynamic properties specifically hydrodynamic flow confinement (HFC) dimensions and diffusive broadening under two-aperture MFPs are determined only through lengthy numerical simulations, or trial and error experiments. Here, we report a complete set of analytical results and scaling laws based on three user-defined parameters that accurately describe all key properties of both microfluidic dipoles (MD) and microfluidic quadrupoles (MQ).

KEYWORDS: Microfluidic probe, open microfluidics, mathematical modeling, mass transfer.

INTRODUCTION

A microfluidic probe (MFP) is a mobile channel-less probe placed closely to the substrate to form a narrow gap into which liquid is injected from a source into the gap and aspirated from another aperture (Figure 1A). By adjusting the injection and the aspiration flow rates, the liquid can be hydrodynamically confined by the surrounding medium [1]. The MFP has many applications, among which are surface gradient generation or analysis and perfusion of organotypic tissue slices [1]. Here, we provide analytical model of the HFC based on the flow ratio α (aspiration flow rate to injection flow rate), the gap size *G* between the MD and the substrate, and the diffusion broadening L_{grad} of the fluid and provide the comparison with the previously published MQ.

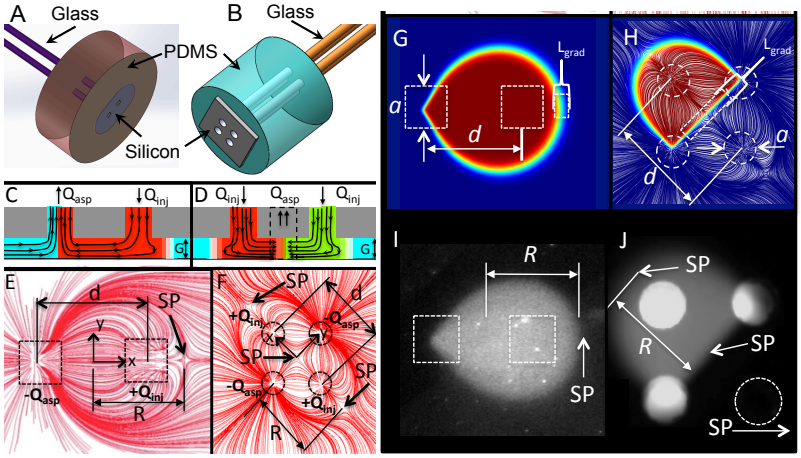

Figure 1 : Advective diffusive transport in both MDs (left column) and MQs (right column). (A-D) 3D operation schematics and side view. (E-F) Flow streamlines and general probe dimensions. The presence of points of zero velocity, or stagnation points (SP), is highlighted. HFC characteristic dimension as described by maximum HFC radius R. (G-H) Finite element simulations of steady state diffusion of a reagent (red) in the computed streamlines (I-J) Typical experimental data showing HFC area. I: d = 50 ∞m, a = 25 ∞m ,Q_{inj} = 0.44 nL/s, and α = 2.5. J: d = 1080 ∞m, a = 360 ∞m, Q_{inj} = 10 nL/s, and α = 10.

METHOD

The three main MFP design criteria – aperture size a, aperture shape (typically square or round), and the interaperture distance d – are linked to the maximum HFC radius R and gradient length scale L_{grad}. 3D finite element simulations of MDs and MQs have been performed using COMSOL, Multiphysics (Burlington, MA). Results for both MDs and MQs are compared with previously published experimental data [2].

RESULTS AND DISCUSSION

Flow velocity

When a low Reynolds number flow is confined between two parallel surfaces forming a narrow gap, a special flow profile arises called Hele-Shaw flow. Hele-Shaw flows are parabolic in the z direction while their height-averaged vector field can be considered irrotational, that is, deriving from a scalar potential function called a velocity potential. In this sense, they are mathematically analogous to 2D electrostatics fields.

$$\boldsymbol{v}(x,y) = -\frac{G^2}{12\eta}\nabla p(x,y) \tag{1}$$

where $p(x,y)$ is the pressure profile, η is the viscosity and G is the gap size. In all cases, for the model to hold, Hele-Shaw condition ($Re \ll 1$, $G^2 \ll d^2$) must be respected. Yet this condition is easily satisfied in the hydrodynamic flow confinement area under a microfluidic probe. In order to compute flow in a more complex situation, we have applied superposition principle by setting two point sources with the flow rates of $Q_{asp}=\alpha Q_{inj}$ located at $r_i = (\pm d/2, 0)$ from center to center of the probes (Fig. 1E). Therefore, we have:

$$\mathrm{v(x,y)} = \frac{\mathrm{Q_{inj}}}{2\pi \mathrm{G}}\left(\frac{(x-d/2)\hat{\mathbf{x}}+y\hat{\mathbf{y}}}{(x-d/2)^2+y^2} - \alpha\frac{(x+d/2)\hat{\mathbf{x}}+y\hat{\mathbf{y}}}{(x+d/2)^2+y^2}\right) \tag{2}$$

providing the flow behavior under the MFP except inside the apertures with dimension a [2]. Two orthogonal pairs of sources are located at $r'=(\pm d/2,0),(0,\pm d/2)$ with the same flow ratio, using the same approach, model a microfluidic quadrupole (Fig. 1F).

Stagnation point and HFC analysis

When $\alpha > 1$, there is a point of zero velocity (stagnation point) outside of injection aperture located on the x-axis at a distance R away from center of two probes as shown in Figure 1E. The position of the stagnation point can be obtained by setting $v(R_{MD},0)=0$ in Eq. 2. It is compared in Eq. 3 to the analogous result for microfluidic quadrupoles described elsewhere [2].

$$R_{MD} = \frac{d(\alpha+1)}{2(\alpha-1)}, R_{MQ} = \pm\frac{d}{2}\sqrt{\frac{d(\alpha+1)}{2(\alpha-1)}} \tag{3}$$

Diffusion broadening

Injected reagents in a MFP will circulate within the HFC and be recaptured by the probe, yet diffusion broadening will occur around its as described by the advection-diffusion equation:

$$\frac{\partial C}{\partial t} = D\nabla^2 C - \boldsymbol{v}\cdot\nabla C\,, \tag{4}$$

where C is the relative concentration (0 to 1), D is the species diffusion coefficient, and t is time, and v is found in Eq. 2. To extract the diffusion scale or gradient length L_{grad}, we linearize Eq. 2 around $x = R_{MD}$ and make Eq. 4 dimensionless:

$$\frac{\partial C}{\partial \bar{t}} = \frac{\partial^2 C}{\partial \bar{x}^2} + \bar{x}\frac{\partial C}{\partial \bar{x}}\,, \tag{5}$$

where $\bar{t} = 4DtPe/d^2$, $\bar{x} = 2\sqrt{Pe}(x - R_{MD})/d$, and $Pe = Q_{inj}(\alpha-1)^3/8\pi\alpha DG$. Thus $t_0 = t/\bar{t} = d^2/4DPe$ and $x_0 = (x - R_{MD})/\bar{x} = d/2\sqrt{Pe}$ are the natural time and length scales of the diffusion broadening ($t_0 \approx 0.3s, and\ x \approx 10\ \mu m$ when using the typical experimental conditions described in Fig.

1I.) Figure 2 shows a comparison between numerical experiments and mathematical models to predict both R and L_{grad} for both MDs and MQs. Under the point flow rate assumption ($a/d \ll 1$), the hydrodynamic model described above accurately matches both numerical simulation and experimental data to within 1%. As a/d increases, the error on the model prediction increases, reaching 20% on both R and L_{grad} in the extreme case when $a/d = 0.5$.

Confinement zone in the MDs operation

Controlling the values of R and W is crucial during the MFP's operation as those parameters directly define the shape of the probe's "writing tip". By moving it parallel to the dipole axis, the probe draws the line as shown in Figure 3 ($W_{//}$). Conversely, moving perpendicular to the dipole axis gives a brush stroke of thickness:

$$W_{\perp} = d/2 + R_{MD} = \frac{\alpha d}{\alpha - 1} \tag{6}$$

Likewise, similar analysis can be obtained for the MQ to provide the probe's effective brush stroke in surface patterning:

$$W_{\parallel} = d, W_{\perp} = cR_{MQ} = \frac{cd}{2}\sqrt{\frac{\alpha+1}{\alpha-1}} \tag{7}$$

where c is the constant and has the value of c=1 when the fluid is injected in one of the injection probe and c=2 when fluid is injected in both injection probes as shown in Figure 1F. If the probe tilted with the angle θ, using simple superposition rule we can calculate the width of the trait by:

$$W_{eff}(\alpha) = W_{\parallel}(\alpha)\cos\theta + W_{\perp}(\alpha)\sin\theta \tag{8}$$

It is worth to note that in the current analysis, the effective shape of the stroke in Eq. 8 omits the reagent's diffusion length in the MFP operation. It also assumes that the probe moves at a velocity much lower than the fluid velocity inside the MFP. The diffusion length varied with respect to $Pe^{1/2}$ [2].

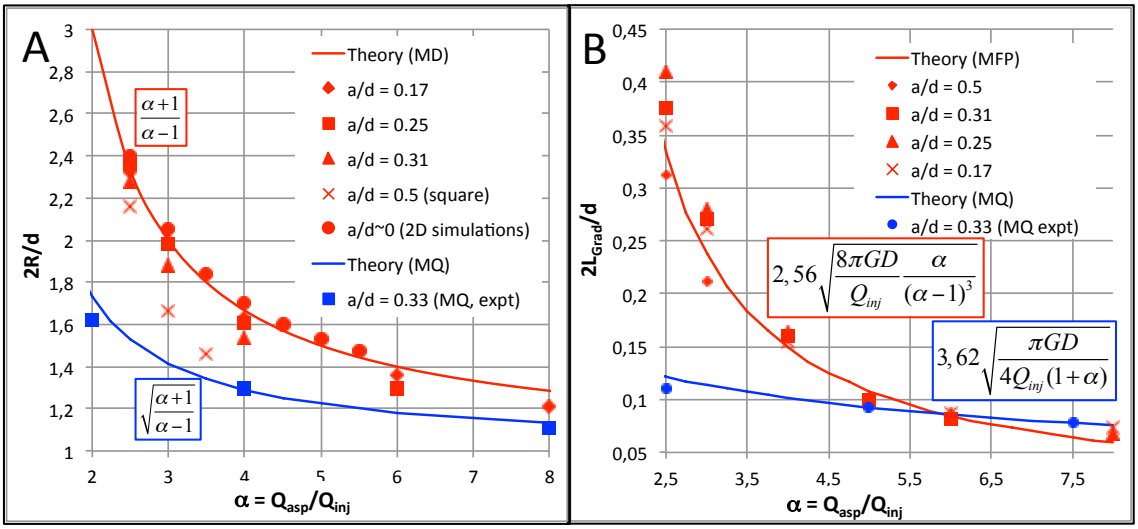

Figure 2. Theoretical predictions for HFC and gradient length of MD (red) and MQ (blue) with respect to flow ratio. Flow rate ratio α and aperture ratio a/d are varied while Q_{inj}, G and D are kept constant. (A) Normalized HFC length 2R/d for both MD and MQ probes. (B) Normalized gradient length $2L_{Grad}/d$ with respect to flow rate ratio α.

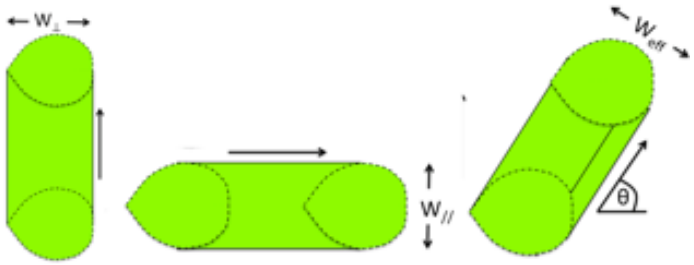

Figure 3: MFP operation parameters such as the brush stroke can be modeled as a linear combination of maximum probe dimension parallel and perpendicular to probe displacement.

Shear stress plays an important role in biological event as it has direct effect on cellular/intercellular phenomena. In Hele-Shaw flow, shear stress is proportional to mean velocity:

$$\tau(x,y)=\frac{6\eta}{G}\vec{v}(x,y)=\tau_0\cdot\tilde{\vec{v}}(\tilde{x},\tilde{y}),\ \tau_0=\frac{6\eta Q_{inj}}{\pi G^2 d} \tag{9}$$

Under typical MFP operating conditions (Fig. 1I), it is thus naturally kept low, i.e. in the < 1 Pa range. Table 1 summarizes the various scaling laws obtained.

Table 1. *Derived scaling laws for microfluidic probes operated within the Hele-Shaw flow regime.*

Criteria	Formula MD	Formula MQ	Description
Maximum HFC radius (*R*)	$R=\frac{d}{2}\left(\frac{\alpha+1}{\alpha-1}\right)$	$R=\frac{d}{2}\sqrt{\frac{\alpha+1}{\alpha-1}}$	*HFC maximum width*
Péclet Number (Pé)	$Pé=\frac{Q_{inj}}{8\pi DG}\frac{(\alpha-1)^3}{\alpha}$	$Pé=\frac{4Q_{inj}(1+\alpha)}{\pi GD}$	*Diffusive broadening*
Diffusion length scale (DL)	$DL\propto\frac{d}{\sqrt{Pé}}$	*idem*	*Concentration gradient lengths*
HFC response time (t)	$t\propto\frac{d^2}{Pé D}$	*idem*	*HFC settling time after an adjustment*
Shear stress (τ)	$\tau=\frac{6\eta\vec{v}}{G}$	*idem*	*Flow-induced surface shear stress*
Max Shear stress (τ_{max})	$\tau_{max}\approx\alpha\tau_0 d/a$ (round) $\tau_{max}\approx 0.86\alpha\tau_0 d/a$ (square) $\tau_0=\frac{6\eta Q_{inj}}{\pi G^2 d}$	*idem* *idem*	*Maximal flow-induced surface shear stress under probe*

CONCLUSION

The current analytical model yields simple equations that accurately predict all major hydrodynamic parameters of MFPs (Table 1), and will help in the on-going effort to rationalize design and automate MFP operation, such as MFP brush stroke according to writing angle as well as the gradient steepness at stagnation points [4]. These equations will help to advance the field of MFPs, and might be extended to the analysis of MFPs under lateral geometry [5].

REFERENCES

[1] Qasaimeh et al., "Microfluidic probes for use in life sciences and medicine", *Lab Chip*, 13, 1, 40–50, 2013.

[2] Qasaimeh et al., "Microfluidic quadrupole and floating concentration gradient", *Nat. Commun.*, 2, 464, 2011.

[3] Juncker et al., "Multipurpose Microfluidic Probe", *Nat. Materials*, 4, 622–628, 2005.

[4] Cors et al., "A compact and versatile microfluidic probe for local processing of tissue sections and biological specimens", *Rev. Sci. Instrum.*, 85, 3, 034301, 2014.

[5] Sarkar et al.,"Microfluidic probe for single-cell analysis in adherent tissue culture" *Nat. Commun.*, 5, 3421, 2014.

CONTACT

* Thomas Gervais; Thomas.Gervais@polymtl.ca phone: +1 514 340-4711 Ext 3752;